



RESEARCH

Dynamics and multi-scale modeling with time delays for three stages of synaptic facilitation

Lijie Hao · Zhuoqin Yang

Received: 12 January 2024 / Accepted: 16 March 2024 / Published online: 15 April 2024
© The Author(s), under exclusive licence to Springer Nature B.V. 2024

Abstract Serotonin-induced facilitation of synaptic transmission at the sensorimotor synapse in *Aplysia* occurs in three temporal phases: short-term facilitation (STF), intermediate-term facilitation (ITF), and long-term facilitation (LTF). The delayed onset of LTF is considered to be related to the time-consuming processes of transcription and translation in protein synthesis. In this work, we develop a multi-scale mathematical model that involves gene transcription and protein synthesis with time delays, presynaptic membrane potential, and excitatory postsynaptic potential for the three stages of synaptic facilitation. The positive feedback loop that forms the basis of bistability according to our bifurcation analysis may account for the transition between two different states following stimulations. Our model simulates experimental findings on the generation of STF, ITF and LTF under different applications of 5HT stimulation. We further confirm that ITF is dependent on translation, whereas LTF relies on both translation and transcription. In addition, we find that the threshold of the number of repeated pulses of 5HT required for the induction of LTF changes with different ranges of the time delays. Our model could provide a useful framework for exploration of dynamical

mechanisms of different temporal domains of synaptic plasticity, as well as guiding investigations into other processes underlying memory formation.

Keywords Synaptic facilitation · Temporal phases · Multi-scale modeling · Dynamical analysis

1 Introduction

Learning and memory are two of the most magical capabilities of our minds and have attracted intense interest in neuroscience research [1–5]. It is well established that memories can exist in many different temporal domains ranging from short-term memory (lasting seconds to minutes) to long-term memory (lasting days, weeks, or even a lifetime) [6]. Considerable biological research has been devoted to identifying the temporal dynamics of different phases of memory [7]. For example, the gill withdrawal reflex of the marine mollusk *Aplysia* is known to exhibit sensitization after a stimulus such as tail shock, providing an experimental system that is useful in delineating possible cellular mechanisms contributing to memory storage [8,9].

Under stimulation by different serotonin (5HT) exposures, the sensitization memory of *Aplysia* displays three temporally and mechanistically distinct phases of synaptic facilitation of sensory neuron to motor neuron (SN-MN) synapses: short-term facilitation (STF), intermediate-term facilitation (ITF), and long-term facilitation (LTF) [10,11]. A single brief

L. Hao
School of Mathematics Science, Tianjin Normal University,
Tianjin 300387, China

Z. Yang (✉)
School of Mathematical Sciences, Beihang University, Beijing
100191, China
e-mail: yangzhuoqin@buaa.edu.cn

exposure of 5HT produces only STF (lasting <30 min) independent of gene expression. However, five spaced applications of 5HT induce not only ITF (lasting 1–3 h), which depends exclusively on translation but not transcription, but also LTF (lasting > 24 h), which requires both protein and RNA synthesis [6, 12].

In the induction of ITF by 5HT at SN-MN synapses, activation of protein synthesis in the presynaptic neuron requires release of an *Aplysia* neurotrophin (ApNT), an invertebrate ortholog of the vertebrate brain-derived neurotrophic factor (BDNF) [13]. ApNT released from the presynaptic neuron stimulates protein synthesis in the presynaptic neuron via activation of phosphatidylinositol 3-kinase (PI3K)/Akt as well as mitogen-activated protein kinase (MAPK) signaling downstream of presynaptic *Aplysia* tropomyosin-related kinase (ApTrk) receptors, which eventually forms a feedback loop facilitating the persistence of synaptic plasticity and memory [13]. Positive feedback loop is known to be an essential ingredient for bistability in biochemical systems [14]. Following a brief stimulation, the system may switch from a low state to a high state at a bifurcation point as the system has two stable steady states. Therefore, bistability caused by a positive feedback loop is critical for the sustained high levels of key proteins in the system for the establishment of long-term memory [15].

According to the hypothetical time courses of the three different phases of facilitation produced by 5HT exposure, ITF overlaps with the decay of STF but not with LTF, as it decays to baseline within 3 h after 5HT application, that is, several hours prior to the onset of LTF (10–15 h) [6, 16]. Moreover, LTF is not a simple continuation of ITF but develops separately with much slower kinetics. The time delay in the expression of LTF reflects the total time required for 5HT-induced protein synthesis, subsequent transport of proteins to the SN terminal region, and induction of structural changes at the synapse [6]. As LTF induction requires gene expression, which involves a series of steps including binding of transcription factors to DNA, gene transcription, and translation in ribosomes, it is necessary to take into account the role of time delays in processes such as transcription and translation to understand the delayed onset of LTF.

To gain insight into the induction of the different temporal phases of synaptic facilitation following 5HT exposure, it is essential to characterize the dynamics of biochemical signaling cascades downstream of

the stimulus. Mathematical models associated with the gill withdrawal reflex in *Aplysia* mainly depict processes at a synaptic or molecular level [15, 17–22]. To describe the dynamics of synaptic transmission at the SN-MN connection mediating the reflex, Gingrich and Byrne propose a model (G–B model) consisting of two pools of vesicles representing neurotransmitter release from the sensory neuron to predict features of synaptic depression in *Aplysia* [17]. Zhou et al. modify the G-B model by incorporating a new term for PKC-dependent vesicle mobilization process to explore the contribution of PKC to 5HT-induced STF [19]. Hao and Yang build a multi-scale mathematical model integrating regulation of gene transcription, local translation, and membrane action potential in the presynaptic sensory neuron with the excitatory postsynaptic potential (EPSP) to investigate the mechanisms underlying the synapse specificity of LTF in *Aplysia* [15]. In view of the different stages of memory, Pettigrew et al. develop a model to examine dynamical properties of regulatory motifs correlated with the three temporal domains of facilitation of the *Aplysia* SN-MN synapse [18]. However, their model does not consider the process of presynaptic translation regulated by ApNT/ApTrk signaling, which has a critical role in the transition from STF to ITF. Owing to the complexity of the learning-related neuronal system, the dynamical mechanisms of transitions between the stages of synaptic plasticity are poorly understood.

In the present study, our primary focus is to illuminate the cellular and molecular mechanisms underlying transitions from STF to ITF and LTF induced by 5HT. We construct a multi-scale mathematical model with two time delays for the SN-MN synapse that encompasses gene transcription, protein synthesis, and membrane potential in the presynaptic neuron, as well as EPSP. Model simulations exhibit three distinct temporal domains of synaptic facilitation, and depict the dynamics of levels of molecules as a basis for the induction of the three stages of memory. Through inhibition of translation and transcription, we elucidate the roles of protein and mRNA synthesis in transitions from STF to ITF and from ITF to LTF. Furthermore, we show that the threshold of the number of repeated 5HT pulses for LTF increases with the total time delays in the system. This model may serve as a template for investigation of dynamical mechanisms of biochemical processes underlying different phases of memory.

2 Model and methods

2.1 Model description

At SN-MN synapses in *Aplysia*, five pulses of 5HT induce ITF and LTF, whereas one pulse induce only STF [10,11]. Experiments demonstrates that STF is independent of gene expression, ITF depends on translation but not transcription, and LTF requires both protein and RNA synthesis [6,12]. At molecular level, activation of protein kinase A (PKA) is an important mode of intracellular signaling in *Aplysia* sensory neurons. The transient activation of PKA by 5HT is critical for STF, whereas more prolonged activation leads to nuclear translocation of the catalytic subunit where it activates a transcriptional cascade required for LTF [11]. Based on the experimental studies, a model is developed to explore dynamical mechanisms underlying the induction of three different temporal domains of facilitation.

Figure 1 shows signaling pathways involved in synaptic facilitation between sensory neurons and motor neurons in *Aplysia*. 5HT activates PKA via an increase in presynaptic cyclic AMP (cAMP), and causes dissociation of the regulatory subunits and catalytic subunits of PKA [23]. The active catalytic subunit of PKA, in turn, phosphorylates the K^+ channel to reduce specific K^+ currents and broaden the action potential, allowing greater Ca^{2+} influx into the presynaptic terminal with each action potential [23]. Subsequently, the greater Ca^{2+} influx facilitates transmitter (glutamate) release and increases EPSP, a measure of the effectiveness of the synapse between the sensory neuron and the motor neuron [24]. Serotonin activates PKA, which leads to synaptic strengthening through enhanced glutamate (Glu) release produced by greater Ca^{2+} influx.

Active PKA can also activate the transcriptional activator CREB1, which in turn induces the transcription of ApNT necessary for PKA activity. In addition, activation of presynaptic PKA enhances ApNT from the presynaptic neuron to promote local protein synthesis. The catalytic subunits translocate to the nucleus and phosphorylate and activate transcription factor CREB1 to trigger gene expression [23]. In mammalian neurons, the BDNF [25–27] promoter contains the CREB binding site CRE, which allows activated CREB to promote the transcription of BDNF [28,29]. Research on ApNT expression reveals a high level of expression

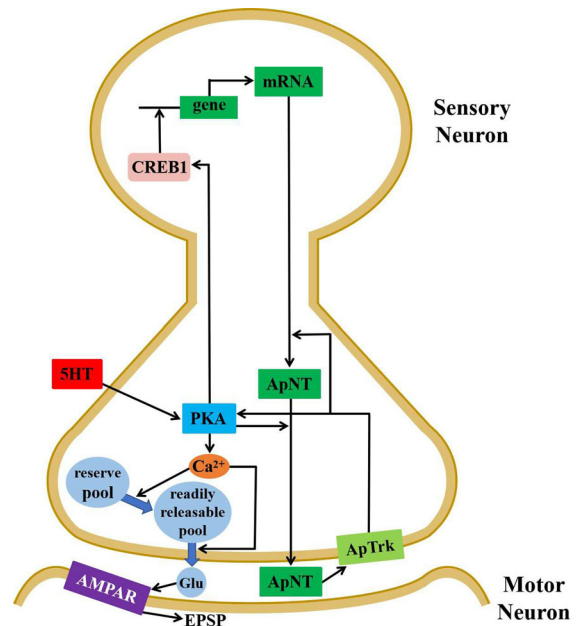


Fig. 1 Signaling pathways involved in synaptic facilitation

restricted to the presynaptic sensory neurons at the SN-MN synapse, which is consistent with the axonal localization of BDNF in the mammalian central nervous system (CNS) [13]. As *Aplysia* neurotrophin is well conserved with vertebrate neurotrophins, we assume that CREB1 can induce ApNT gene transcription in the sensory neuron. In addition, activation of presynaptic PKA produces an increase in the release of ApNT from the presynaptic neuron that in turn acts on presynaptic ApTrk receptors and activates downstream signaling including PKA, suggesting a positive feedback loop [13,30]. The released ApNT also stimulates protein synthesis, which is thought to replenish the reserve vesicle pool and other synaptic proteins that support release of neurotransmitters from the presynaptic neuron [13]. Therefore, we further assume that presynaptic ApNT protein synthesis is regulated by ApNT and ApTrk signaling.

It is known from experiments that ITF decays within 3 h after 5HT application, but LTF is not expressed until 10 h after 5HT exposure [6]. The delayed onset of LTF is primarily due to the time needed for protein synthesis. Consequently, time delays should be considered in processes of gene transcription and translation in the model.

For the transmitter release process of the sensory neuron, the synapse contains two pools of vesicles: a

readily releasable pool (RRP) and a reserve pool (RP). Vesicle mobilization from RP to RRP and neurotransmitter release from RRP into the synaptic cleft are regulated by intracellular Ca^{2+} [17, 19].

2.2 Mathematical formulations

The model includes the presynaptic protein synthesis, the presynaptic action potential, and EPSP. We denote the levels of active PKA, CREB1, ApNT mRNA, and presynaptic ApNT protein by [PKA], [CREB1], [mRNA], and [ApNT], respectively. The activity of presynaptic PKA is regulated by serotonin and ApNT, expressed as $\alpha[5HT]$ and $\frac{\gamma[ApNT]}{[ApNT]+K_3}$, respectively. The rate of CREB1 activation promoted by PKA is presented as a linear function of [PKA] with a coefficient of λ . As suggested by experimental results, it is possible that the delayed onset of LTF can be attributed partly to the time needed for new protein synthesis induced by 5HT stimulation [6]. We assume that transcription of the ApNT gene and translation of ApNT mRNA are respectively regulated by the transcriptional activator CREB1 and extracellular ApNT; however, time delays τ_1 in the transcription process and τ_2 in the translation process are introduced in our formulations. As a result, CREB1 controls ApNT mRNA synthesis through a Hill-type function $\frac{\beta[CREB1]_{\tau_1}^2}{[CREB1]_{\tau_1}^2 + K_2^2}$, where a Hill coefficient of 2 for [CREB1] represents the requirement for two CREB1 monomers to form homodimers. In light of the dependence of ApNT secretion on presynaptic PKA, the synthesis rate of ApNT protein is given by $[mRNA]_{\tau_2}(\theta + \frac{\delta[ApNT]}{[ApNT]+K_3})(k_e + k_p[PKA])$. Furthermore, ω denotes the basic transcription rate of the ApNT gene, and μ and ρ define basal activation rates of presynaptic PKA and CREB1, respectively. Degradation rates of PKA, CREB1, ApNT mRNA, and ApNT protein are represented by $d_1, d_2, d_3,$ and $d_4,$ respectively. The dynamics of these molecular concentrations are given by differential equations (1)–(4).

$$\frac{d[PKA]}{dt} = \mu + \alpha[5HT] + \frac{\gamma[ApNT]}{[ApNT] + K_3} - d_1[PKA], \tag{1}$$

$$\frac{d[CREB1]}{dt} = \rho + \lambda[PKA] - d_2[CREB1], \tag{2}$$

$$\frac{d[mRNA]}{dt} = \omega + \frac{\beta[CREB1]_{\tau_1}^2}{[CREB1]_{\tau_1}^2 + K_2^2} - d_3[mRNA], \tag{3}$$

$$\frac{d[ApNT]}{dt} = [mRNA]_{\tau_2}(\theta + \frac{\delta[ApNT]}{[ApNT] + K_3}) - (k_e + k_p[PKA]) - d_4[ApNT]. \tag{4}$$

Equations for the action potential of the presynaptic neuron are based on the Morris–Lecar (ML) model [31] and are formulated as:

$$C \frac{dV}{dt} = -g_L(V - V_L) - g_{Ca}m_{\infty}(V - V_{Ca}) - g_K n(V - V_K) + I_0, \tag{5}$$

$$\frac{dn}{dt} = (n_{\infty} - n)/\tau_n, \tag{6}$$

$$\frac{dg_K}{dt} = g_{K0} - \frac{k_g[PKA]^2}{K_g^2 + [PKA]^2}g_K - d_k g_K. \tag{7}$$

Here, V is the membrane potential of the presynaptic neuron. As the catalytic subunit of PKA may cause phosphorylation of the K^+ channel, we assume that the conductance of the presynaptic K^+ channel (g_K) is dependent on PKA activity in Eq. (7). According to the ML model, the presynaptic Ca^{2+} current can be represented by the following formulation.

$$I_{Ca} = -g_{Ca}m_{\infty}(V - V_{Ca}). \tag{8}$$

The gating variables $m_{\infty}, n_{\infty},$ and τ_n are

$$m_{\infty} = \frac{1}{2}(1 + \tanh((V - v_1)/v_2)), \tag{9}$$

$$n_{\infty} = \frac{1}{2}(1 + \tanh((V - v_3)/v_4)), \tag{10}$$

$$\tau_n = \frac{1}{\phi \cosh((V - v_3)/(2v_4))}. \tag{11}$$

The mathematical model of the process of sensory neuron transmitter release is modified from the G-B model of the SN-MN synapse of *Aplysia*, which contains an RRP and an RP of vesicles. In the G-B model, vesicle mobilization is described by three fluxes: I_S and I_F , which are regulated by the concentration of intracellular Ca^{2+} , represent the slow and fast fluxes from RP to RRP, respectively; and I_{VD} is a flux driven by differences in concentration between vesicles in the RRP and RP [17, 19]. Furthermore, the RP is refilled by a flux of vesicles I_N , and the flux of vesicles during an action potential from RRP into the synaptic cleft is represented by I_R .

In the present model, the dynamics of the pools of vesicles, regulation of intracellular Ca^{2+} concentration, synaptic transmission, and vesicle mobilization from RP to RRP are described by the following equations:

$$\frac{dC_R}{dt} = (I_F + I_S + I_{VD} - I_R) \cdot \frac{1}{V_R}, \tag{12}$$

$$I_R = (C_R \cdot V_R) \cdot ((I_{Ca}/K_{C1}) \cdot K_R), \tag{13}$$

$$I_{VD} = (C_F - C_R) \cdot K_{VD}, \tag{14}$$

$$I_F = \frac{C_F}{C_{Fl}} \cdot \frac{K_F}{1 + \frac{M_F}{C_C^{N_F}}}, \tag{15}$$

$$I_S = \frac{C_F}{C_{Fl}} \cdot PVM_S, \tag{16}$$

$$I_N = (C_{Fl} - C_F) \cdot K_N, \tag{17}$$

$$\frac{dPVM_S}{dt} = \left[\frac{K_S}{1 + \frac{M_S}{C_C^{N_S}}} - PVM_S \right] \cdot \frac{1}{T_S}, \tag{18}$$

$$\frac{dC_F}{dt} = (I_N - I_F - I_S - I_{VD}) \cdot \frac{1}{V_F}, \tag{19}$$

$$\frac{dC_C}{dt} = ((I_{Ca}/K_{C2}) - I_U - I_D) \cdot \frac{1}{V_C}, \tag{20}$$

$$I_U = \frac{K_U}{1 + M_U/C_C^2}, \tag{21}$$

$$I_D = C_C \cdot K_D. \tag{22}$$

Here, C_R and C_F are the concentrations of vesicles in the RRP and RP, respectively. C_{Fl} is the steady-state value of C_F , C_C the Ca^{2+} concentration in the interior Ca^{2+} compartment, and V_C the volume of the interior Ca^{2+} compartment. K_R , K_N , K_{C1} , K_{C2} , and K_{C3} are constants. I_U is a Ca^{2+} flux that removes Ca^{2+} from the cytosol owing to active uptake leading to sequestration or removal from the cell by organelles such as the endoplasmic reticulum and mitochondria, and I_D is a flux that removes Ca^{2+} owing to diffusion into compartments that are not modeled. K_F and K_S are the rate constants, M_F and M_S the concentration constants, N_F and N_S the Hill coefficients, K_{VD} and K_D the diffusion constants, and V_R and V_F the volumes of the RRP and RP, respectively. PVM_S is the potential for vesicular mobilization of I_S . T_S is the time constant, K_U the constant for Ca^{2+} uptake, and M_U the concentration constant for Ca^{2+} uptake. Assuming that the rate of increase of the EPSP is proportional to the total amount of transmitter released during a stimulus, the EPSP can be described by the following differential equation:

$$\frac{dEPSP}{dt} = (C_R \cdot V_R) \cdot (I_{Ca} \cdot K_R) - vEPSP, \tag{23}$$

where v is the rate of decrease of the EPSP. For details of the release process model, refer to the G-B model [17, 19].

The default parameter values used in this study are listed in Table 1. The estimation of parameter values is mainly based on previous models [15, 17, 19, 31], and

parameters unavailable from the published literatures are set to fit the experimental data.

2.3 Methods

In experiments, one to three pulses of 5HT induces short-term (minutes) PKA activation, four to five pulses induce intermediate-term (3 h) activation, and five pulses induce long-term (> 20 h) persistent activation [7]. To realize distinct phases of PKA activation, we perform synapse stimulations of one, three, four, and five pulses of 10 μ M 5HT for 5 min, with an inter-pulse interval (from the end of one pulse to the onset of the next) of 15 min to the synapse. In computations, the stimulations are designed as follows to ensure the end time of each stimulation programme is at the zero point:

- 1 \times 5HT: one pulse of 10 μ M 5HT is applied to the synapse beginning at $t = -5$ min;
- 3 \times 5HT: three pulses of 10 μ M 5HT are applied to the synapse beginning at $t = -45$ min;
- 4 \times 5HT: four pulses of 10 μ M 5HT are applied to the synapse beginning at $t = -65$ min;
- 5 \times 5HT: five pulses of 10 μ M 5HT are applied to the synapse beginning at $t = -85$ min.

In the numerical simulations, bifurcation analyses are performed with XPPAUT, and differential equations are solved using the Runge-Kutta method [32]. Simulations for EPSP are performed with MATLAB using the Euler scheme with a time step of 0.1 ms.

3 Results

3.1 The reversible and irreversible bistable switches of the positive feedback loop

In the model, active presynaptic PKA promotes ApNT gene transcription via CREB1 and increases release of ApNT from the presynaptic neuron, which in turn acts on presynaptic ApTrk receptors and activates PKA to form a positive feedback loop. From the perspective of dynamics, a positive feedback loop is usually associated with bistability essential for maintaining high levels of molecules. Therefore, we perform bifurcation analysis to explore the existence and transitions of steady states based on the positive feedback loop in the system.

Table 1 Default parameter values of Eqs. (1)–(23)

Parameter	Value	Source	Parameter	Value	Source
[5-HT] (μM)	0		μ ($\mu\text{M min}^{-1}$)	0.0004	
α (min^{-1})	0.118		γ ($\mu\text{M min}^{-1}$)	0.5	
d_1 (min^{-1})	0.15		ρ (μM)	0.001	
λ (min^{-1})	0.16		d_2 (min^{-1})	0.2	
ω ($\mu\text{M min}^{-1}$)	0.008		β ($\mu\text{M min}^{-1}$)	0.064	
K_1 (μM)	0.8		d_3 (min^{-1})	0.004	
K_2 (μM)	4		τ_1 (h)	3	
δ (min^{-1})	0.02		K_3	0.45	
d_4 (min^{-1})	0.08		θ (min^{-1})	0.000004	
k_e (min^{-1})	0.6		k_p ($\text{min}^{-1} \mu\text{M}^{-1}$)	0.78	
τ_2 (h)	3		k_g (min^{-1})	0.115	
K_g (μM)	0.5		g_{K0} ($\text{mS/cm}^2 \text{min}^{-1}$)	1.3	
d_K (min^{-1})	0.12		C ($\mu\text{F/cm}^2$)	20	[31]
g_L (mS/cm^2)	2	[31]	g_{Ca} (mS/cm^2)	4	[31]
V_L (mV)	-50	[31]	V_{Ca} (mV)	100	[31]
V_K (mV)	-70	[31]	v_1 (mV)	-1	[31]
v_2 (mV)	15	[31]	v_3 (mV)	10	[31]
v_4 (mV)	14.5	[31]	ϕ (ms^{-1})	0.06667	[31]
v (ms^{-1})	0.02	[15]	I_0 ($\mu\text{A/cm}^2$)	35	[15]
K_{C1} ($\mu\text{A/cm}^2$)	10^6	[15]	K_{C2} ($\mu\text{A/cm}^2$)	1	[15]
K_{C3} ($\text{mS/cm}^2 \text{ms}$)	10^6	[15]	M_U	790	[17]
K_D	0.338	[17]	K_{VD}	0.001	[17]
C_{Fl}	100	[17]	N_F	2.83	[17]
N_S	1.75	[17]	T_S	213	[17]
K_N	0.005	[17]	V_F	6.08	[17]
V_C	2.15	[17]	V_R	1	[17]
K_F	21	[17]	K_S	35	[17]
M_F	0.0008	[17]	M_S	0.075	[17]
K_R	3.16	[17]	K_U	2907	[17]

We first consider a two-parameter bifurcation diagram for the stimulus strength [5HT] and the positive feedback strength γ , as shown Fig. 2a. The parameter plane ([5HT], γ) is divided into a bistable region (yellow region) and a monostable region (green region) by the saddle-node bifurcation curves (black curves) SN1 and SN2 from the codimension-2 cusp point (CP). The dynamics of the system as [5HT] changes may thus exhibit a reversible switch when $\gamma < 0.4 \mu\text{M min}^{-1}$ (below the magenta dashed line in Fig. 2a) and an irreversible bistable switch when $\gamma > 0.4 \mu\text{M min}^{-1}$ (above the magenta dashed line in Fig. 2a). We further examine the bistable behaviors under 5HT stimulation

to simulate experimental data through one-parameter bifurcation analysis with respect to [5HT] for fixed γ . Bifurcation diagrams for [PKA] (blue curves) and g_K (red curves) versus [5HT] are illustrated in Fig. 2b, c for two different values of γ , 0.35 and 0.5, respectively. When $\gamma = 0.35 \mu\text{M min}^{-1}$, there is a reversible switch of bistability between the two saddle-node bifurcation points (SN1 and SN2), such that [PKA] increases during stimulation and decreases rapidly to a low stable state after the stimulation with 5HT (see Fig. 2b). When $\gamma = 0.5 \mu\text{M min}^{-1}$, only one saddle-node bifurcation point (SN1) is located in the physiological range of the parameter, so the bifurcation diagram shows an irre-

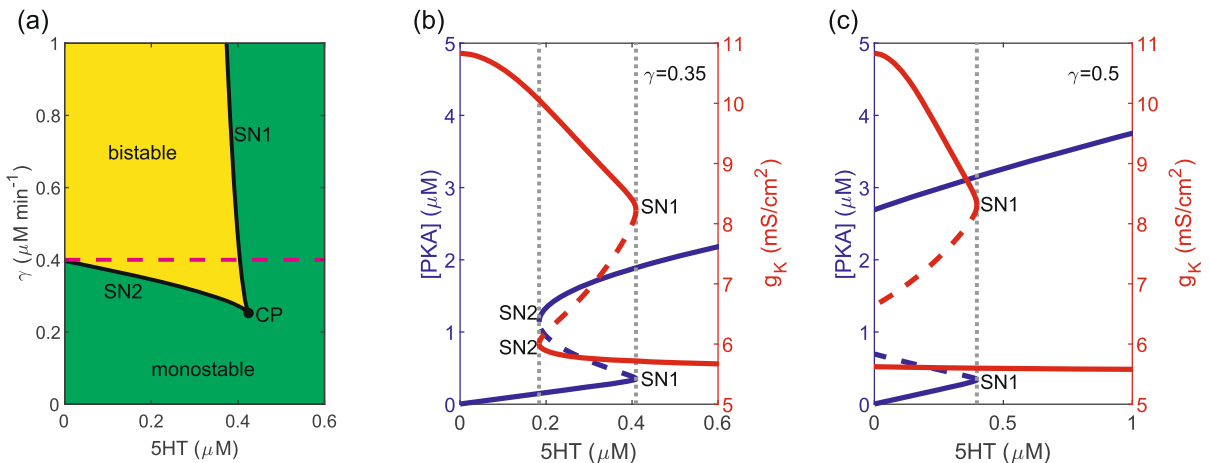


Fig. 2 Bifurcation diagrams of the system with $\tau_1 = \tau_2 = 0$ h. **a** Two-parameter bifurcation diagram in the ([5-HT], γ) plane. Black curves depict the loci of the saddle-node bifurcation points.

b Bifurcation diagrams of [PKA] (blue) and g_K (red) versus [5-HT] at $\gamma = 0.35 \mu\text{M min}^{-1}$. **c** Bifurcation diagrams of [PKA] (blue) and g_K (red) versus [5-HT] at $\gamma = 0.5 \mu\text{M min}^{-1}$

versible switch (see Fig. 2c). Thus, [PKA] (g_K) reaches a high (low) level under stimulation with 5HT and permanently remains in the high (low) stable steady state even after the stimulation. The above bifurcation analysis indicates that bistability is critical for maintaining a high level of [PKA], which may have a significant role in the induction of long-term synaptic facilitation and long-term memory.

The phosphorylation by active PKA of the K^+ channel to reduce K^+ currents contributes to presynaptic spike broadening, which in turn improves Ca^{2+} influx to enhance transmitter release and further increases EPSP amplitude [23]. Therefore, we examine the spike duration of presynaptic membrane potential and the amplitude of EPSP for different values of g_K . The time courses of V and EPSP in Fig. 3a1, b1 illustrate that the time durations of the spike become short and EPSP amplitudes gradually decrease as the value of g_K changes from 6 mS/cm² (red) to 7 mS/cm² (yellow), 8 mS/cm² (green), and 9 mS/cm² (blue). Furthermore, we obtain the decreasing trends for both the spike duration of the presynaptic action potential and EPSP amplitude with the increasing g_K , as shown in Fig. 3a2, b2.

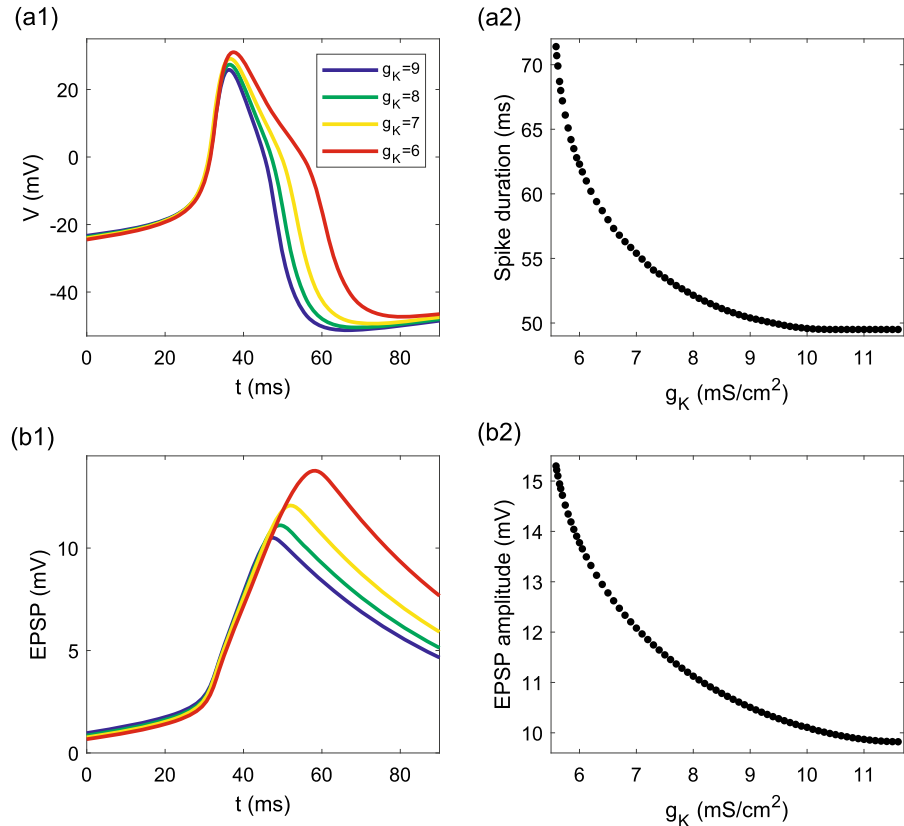
3.2 Induction of short-, intermediate-, and long-term synaptic facilitation under four different 5HT stimulations

3.2.1 Measures of short-, intermediate-, and long-term synaptic facilitation

In the sensory neuron, stimulation using one, three, four, and five pulses of 5HT give rise to three independent phases of PKA activation, which are shown to be correlated with three distinct phases of synaptic facilitation of the SN-MN synapse based on measurements of increases in EPSP [7, 18]. Thus, we next examine the amplitudes of EPSP at 15 min, 2 h and 24 h after stimulation to acquire the induction of STF, ITF, and LTF of the synapse, respectively.

The presynaptic action potential (V) and EPSP are illustrated in Fig. 4. Following one pulse of 5HT stimulation, there are notable increases in the time duration of the presynaptic action potential and amplitude of EPSP at 15 min after stimulation, whereas there is almost no change at 2 h or 24 h after stimulation (see Fig. 4a1–d1). As shown in Fig. 4a2–d2, similar impacts on presynaptic action potential and EPSP are observed following three pulses of 5HT exposure. These findings provide evidence in support of the consensus that both one and three pulses of 5HT stimulation only induce STF. Application of four pulses of 5HT results in significant increases in the spike time duration and ampli-

Fig. 3 Time courses of V (a1) and EPSP (b1) at $g_K = 6$ mS/cm² (red), 7 mS/cm² (yellow), 8 mS/cm² (green), and 9 mS/cm² (blue), respectively. The duration of the presynaptic action potential (a2) and EPSP amplitude (b2) decrease with increasing g_K



tude of EPSP at both 15 min and 2 h but has no effect at 24 h after stimulation (see Fig. 4a3–d3), indicating that four pulses of 5HT stimulation can produce STF and ITF but not LTF. As shown in Fig. 4a4–d4, the spike duration and EPSP amplitude at 15 min, 2 h and 24 h after application of five pulses of 5HT exposure are all markedly elevated, suggesting the generation of STF, ITF, and LTF.

3.2.2 Molecular mechanisms underlying short-, intermediate-, and long-term synaptic facilitation

We further discuss changes at the molecular levels to elucidate molecular mechanisms underlying the three temporal phases of synaptic facilitation. Figure 5a1–a4 shows the time courses of [5HT] in the four stimulus protocols of one, three, four, and five pulses of 5HT exposure. Application of one or three pulses of 5HT only evoke transient PKA activation (see Fig. 5b1, b2), which is not enough to induce high levels of ApNT mRNA and ApNT protein (see Fig. 5c1–d1 and c2–d2).

A minor increase in ApNT provides little feedback to PKA activity, and so PKA has to return to baseline soon after stimulation. Correspondingly, the conductance of the K⁺ channel (g_K) decreases transiently, so short-term increases occur in the spike duration and EPSP amplitude (see Fig. 5e1–g1 and e2–g2).

Four pulses of 5HT enhance PKA activity for several hours, resulting in a temporary elevation of ApNT mRNA and ApNT protein levels, followed by rapid decay (see Fig. 5b3–d3). As a result, the spike duration and the EPSP amplitude increase with decreasing g_K , and then decrease within hours with elevation of g_K (see Fig. 5e3–g3).

Following the application of five pulses of 5HT, [PKA] shows an oscillatory increase for about four hours before returning to its basal level, with a further an elevation of ApNT mRNA levels for about five hours owing to time delays in gene transcription and translation (see Fig. 5b4, c4). Accordingly, the increase in the ApNT protein concentrations activates PKA for about ten hours through positive feedback, such that the low PKA activity increases again and remains at a high

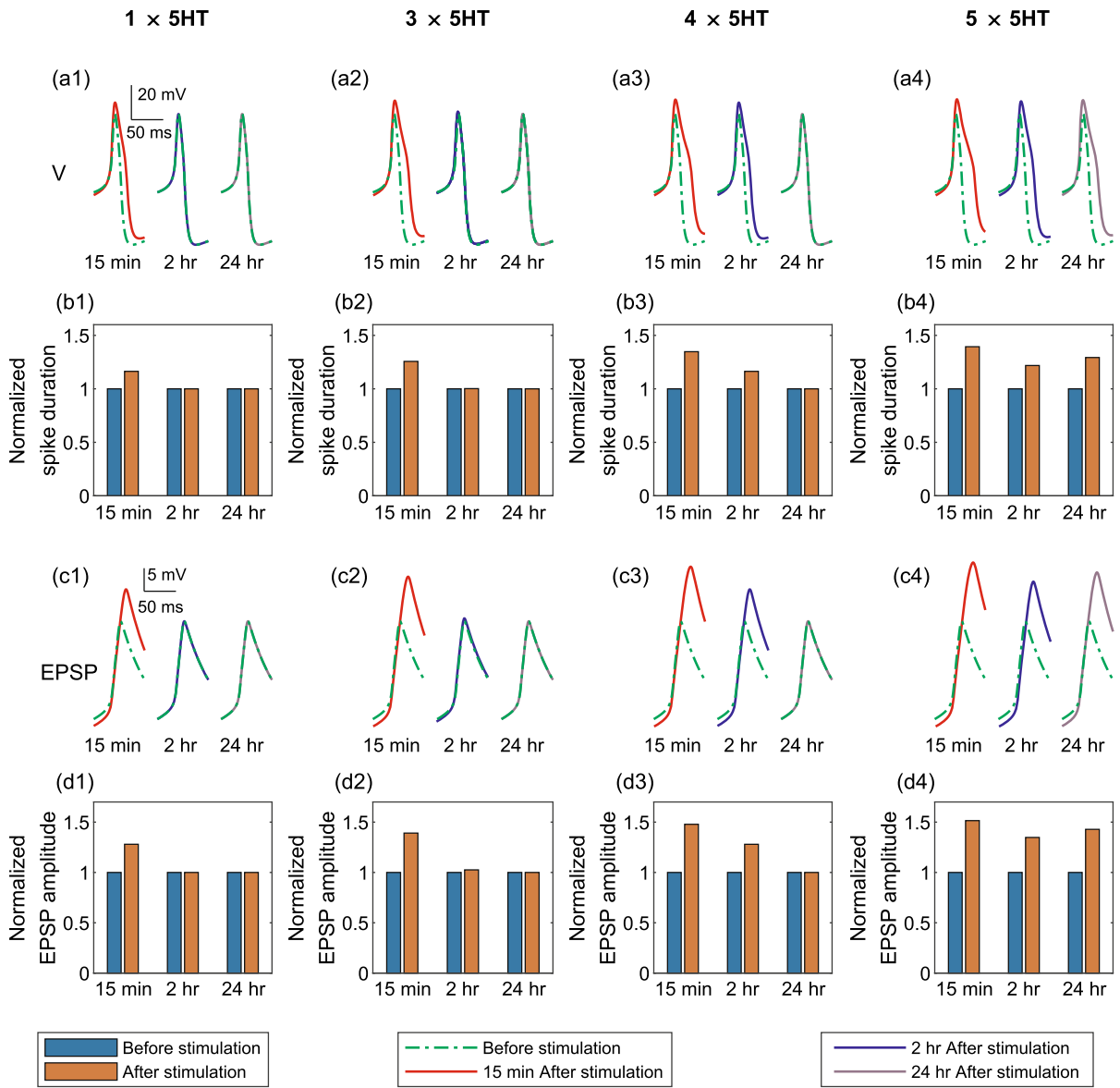


Fig. 4 Presynaptic action potentials and EPSPs following stimulations with one, three, four, and five pulses of 5HT. **a1–a4** Representative presynaptic action potential traces before and after stimulation. **b1–b4** Durations of the action potential, normal-

ized to the spike duration without stimulation, before and after stimulation. **c1–c4** Representative EPSP traces before and after stimulation. **d1–d4** Amplitudes of EPSP, normalized to the EPSP amplitude without stimulation, before and after stimulation

level thereafter (see Fig. 5b4–d4). In addition, the conductance of the K^+ channel decreases to a low level and so both the spike duration and the amplitude of EPSP increase and persist at high levels (see Fig. 5e4–g4).

3.2.3 Sensitivity analysis of short-, intermediate-, and long-term synaptic facilitation to all the parameters

As parameter values can affect system dynamics, it is possible that the simulation results for different phases of synaptic facilitation would change when the

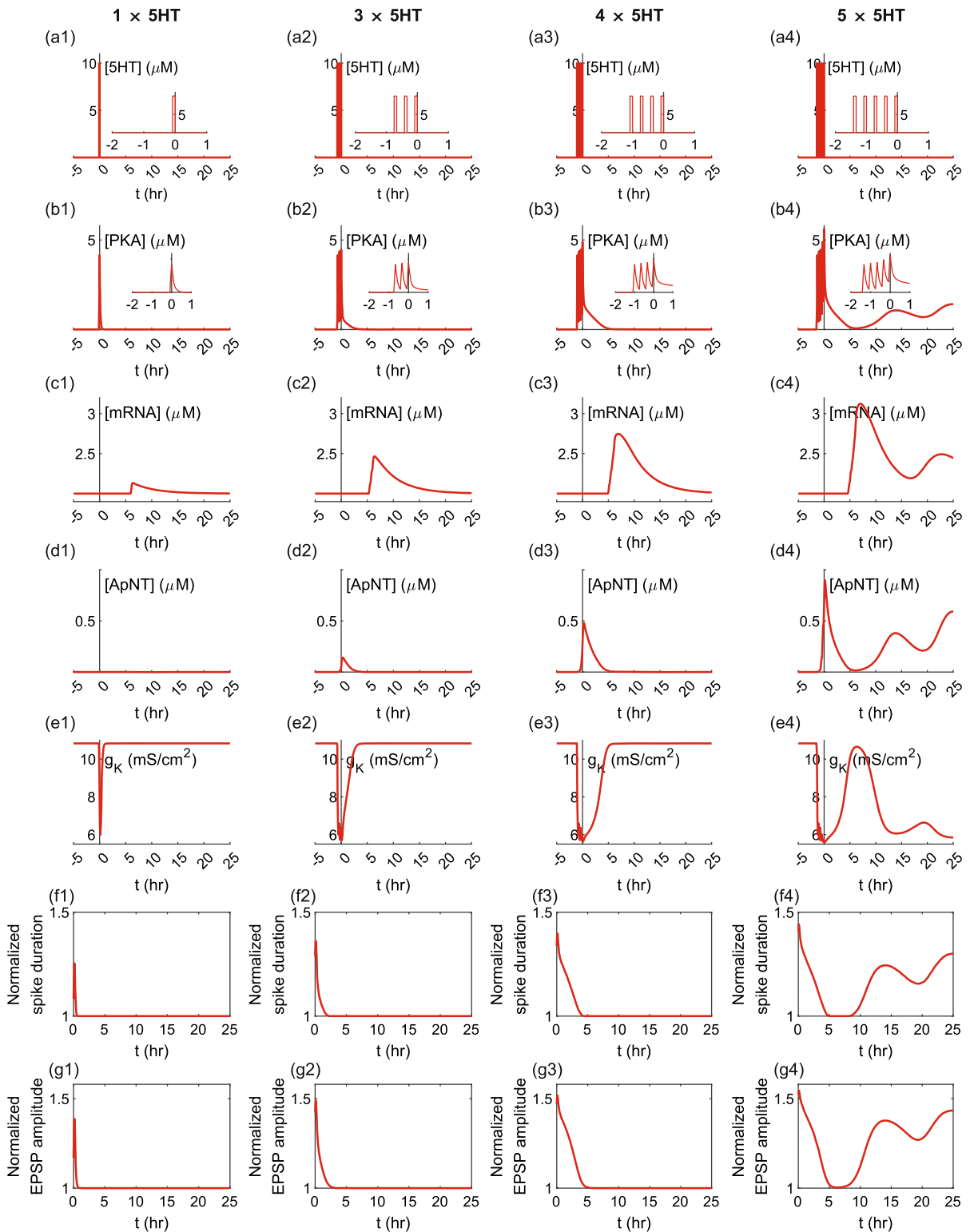
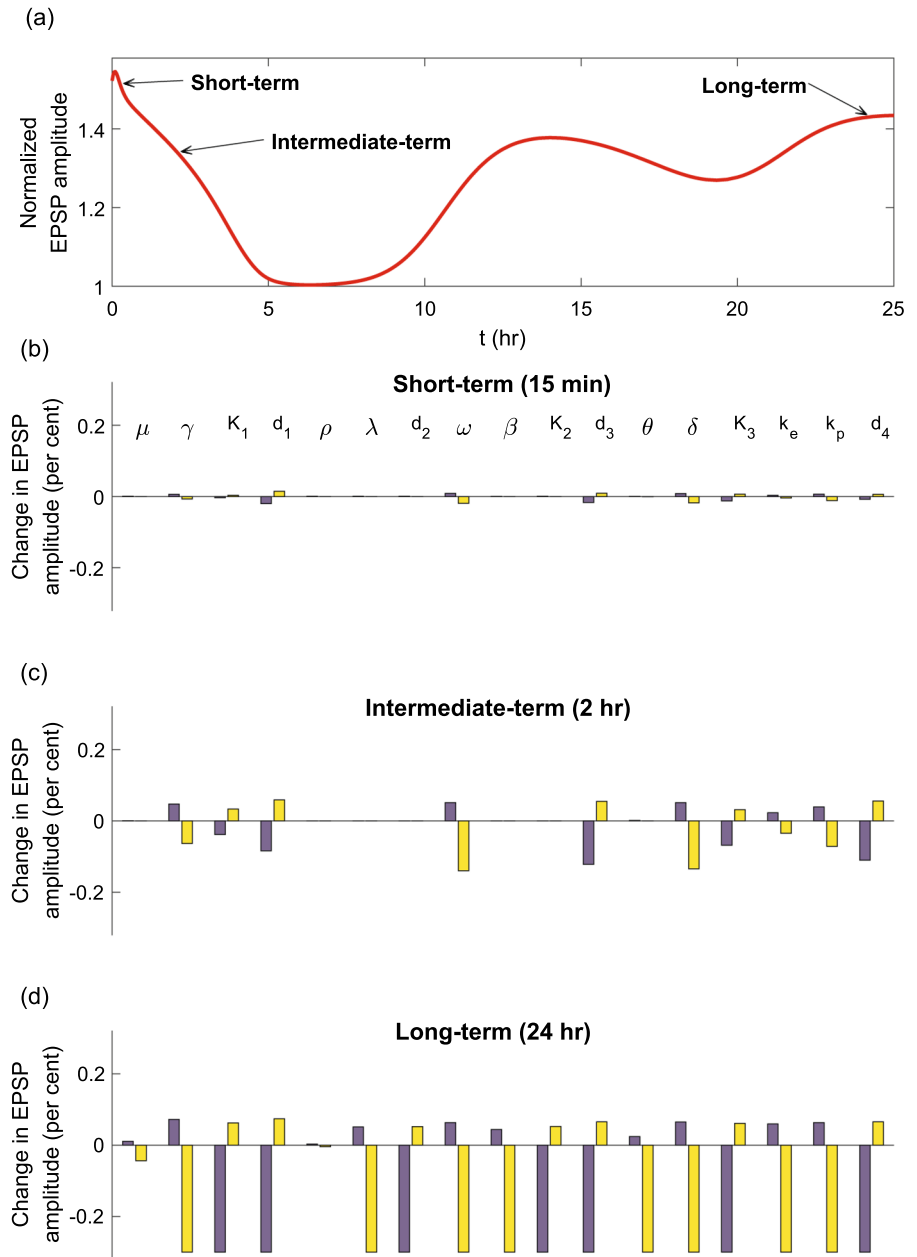


Fig. 5 Time courses of [5HT] (a), [PKA] (b), [mRNA] (c), [ApNT] (d), g_K (e), normalized spike duration (f), and normalized EPSP amplitude (g) after stimulations with one, three, four, and five pulses of 5HT

Fig. 6 Sensitivity of the EPSP amplitude to model parameters. **a** Time course of the normalized EPSP amplitude after stimulation with five pulses of 5HT. **b–d** Percentage change in EPSP amplitude at 15 min, 2 h, and 24 h after five pulses of 5HT



model parameters are varied. To examine the sensitivity of STF, ITF, and LTF to variations in parameter values, we alter each parameter in equations (1)–(4) by 10% and examine changes in EPSP amplitudes at 15 min, 2 h, and 24 h after five pulses of 5HT application (see Fig. 6).

Figure 6a illustrates the time course of normalized EPSP amplitude after stimulation, when all parameters take default values, and indicates the points for sensi-

tivity testing in the three stages of synaptic facilitation. In Fig. 6b–d, each pair of blue bar and yellow bar corresponds to the percentage change in the EPSP amplitude with +10% and –10% changes in parameter values, relative to the case with the default value of one parameter. As shown in Fig. 6b, STF showed low sensitivity to all 17 parameters, as measured by the EPSP amplitude at 15 min after stimulation. ITF, as represented by the EPSP amplitude at 2 h after stimulation, varies

with moderate sensitivity for ten of the parameters and with low sensitivity for the remaining parameters (see Fig. 6c). However, the sensitivity of LTF, as measured by the EPSP amplitude at 24 h after stimulation, is low only for two of the parameters; it is high for all of the other parameters (see Fig. 6d). The high sensitivity of LTF is critical for simulating the threshold pulses of 5HT for the induction of the long-term phase of synaptic facilitation.

In summary, all the results presented above suggest that one or three pulses of 5HT can induce a short-term phase of PKA activity and STF, whereas four pulses of 5HT stimulation can produce an intermediate-term phase of PKA activity and ITF. Moreover, five pulses of 5HT generate both intermediate- and long-term phases of PKA activity, as well as ITF and LTF, with ITF decaying back to baseline several hours before the emergence of LTF. These simulation results obtained with our model are consistent with experimental findings [7]. In addition, STF and ITF are not sensitive to most of the parameters, but LTF is sensitive to almost all parameters.

3.3 Induction of ITF and LTF requires protein and mRNA synthesis

Induction of STF requires neither protein nor RNA synthesis, whereas ITF relies on translation but not transcription, and LTF depends on both transcription and translation [6]. Thereby, we try to verify ITF induced by four or five pulses of 5HT and LTF induced by five pulses of 5HT by inhibiting ApNT protein or mRNA synthesis, when controlling the rate coefficients of translation and transcription δ and β , respectively.

When translation is blocked ($\delta = 0$), the EPSP amplitude is elevated significantly at 15 min but not at 2 h or 24 h after stimulation, as shown in Fig. 7a1, b1, a3, b3; thus, both ITF and LTF are abolished by inhibition of protein synthesis. When transcription is repressed ($\beta = 0$), there is an increase in the amplitude of EPSP at both 15 min and 2 h but not 24 h after stimulation (see Fig. 7a2, b2, a4, b4), suggesting that inhibition of mRNA synthesis only prevents LTF produced by five pulses of 5HT.

We further explore the molecular requirements of ITF and LTF based on the dynamics of the [PKA] concentration and the conductance of the K^+ channel g_K (see Fig. 8). In the case of repression of protein synthe-

sis ($\delta = 0$), transient PKA activation leads to a brief decrease in the conductance of the K^+ channel that can only give rise to a short-term increase in the EPSP amplitude (see Fig. 8a1–c1 and a3–c3). When $\beta = 0$, PKA activity is enhanced, reducing K^+ conductance and elevating the EPSP amplitude for a few hours after four or five pulses of 5HT application (see Fig. 8a2–c2 and a4–c4), implying that ITF can be induced even when the gene transcription process is blocked.

In conclusion, we have confirmed that ITF relies on translation and LTF depends on both translation and transcription, requiring different stages of gene expression.

3.4 Contribution of time delays in transcription and translation to number of pulses of 5HT required for onset of LTF

A long time is required for new mRNA and protein synthesis in the long-term phase of persistent PKA activity, as well as the long-term form of synaptic facilitation, resulting in delayed onset of LTF after spaced exposure to 5HT. Therefore, we explore the effects of time delays τ_1 and τ_2 in the transcription and translation processes on the threshold of the number of pulses required for the long-term phase of PKA activity. Here, we still allow for a pulse of 10 μ M 5HT for 5 min with an inter-pulse interval of 15 min.

As described above, stimulation with three, four, and five pulses of 5HT generate short-, intermediate-, and long-term PKA activation at $(\tau_1, \tau_2) = (3 \text{ h}, 3 \text{ h})$, respectively. Next, we control the time delays τ_1 and τ_2 simultaneously to examine the PKA activity under the three stimulation conditions. As shown in Fig. 9a, three pulses of 5HT exposure causes short-term PKA activation at $(\tau_1, \tau_2) = (4 \text{ h}, 4 \text{ h})$, $(\tau_1, \tau_2) = (3 \text{ h}, 3 \text{ h})$, and $(\tau_1, \tau_2) = (2 \text{ h}, 2 \text{ h})$, but long-term PKA activation when $(\tau_1, \tau_2) = (0 \text{ h}, 0 \text{ h})$. Application of four pulses of 5HT activates PKA for the intermediate-term phase at $(\tau_1, \tau_2) = (4 \text{ h}, 4 \text{ h})$ and $(\tau_1, \tau_2) = (3 \text{ h}, 3 \text{ h})$, but for the long-term phase at $(\tau_1, \tau_2) = (2 \text{ h}, 2 \text{ h})$ and $(\tau_1, \tau_2) = (0 \text{ h}, 0 \text{ h})$ (see Fig. 9b). Following five pulses of 5HT, long-term PKA activation is induced at $(\tau_1, \tau_2) = (3 \text{ h}, 3 \text{ h})$, $(\tau_1, \tau_2) = (2 \text{ h}, 2 \text{ h})$, and $(\tau_1, \tau_2) = (0 \text{ h}, 0 \text{ h})$, whereas the intermediate-term phase of PKA activity appears at $(\tau_1, \tau_2) = (4 \text{ h}, 4 \text{ h})$ (see Fig. 9c). These results indicate that lower (higher) total time lags in the mRNA and protein synthesis

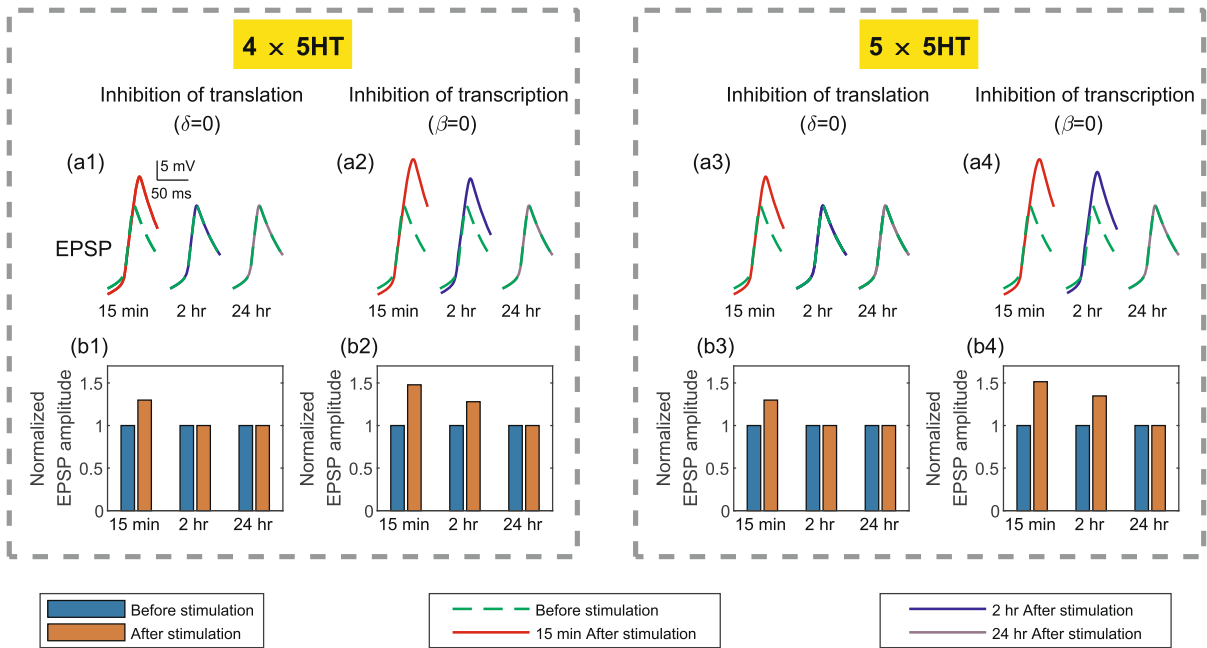


Fig. 7 Presynaptic action potentials and EPSPs following stimulations with four and five pulses of 5HT, with $\delta = 0$ and $\beta = 0$. **a1–a4** Representative EPSP traces before and after stimulation. **b1–b4** Normalized EPSP amplitudes before and after stimulation

processes decrease (increase) the number of repeated pulses of 5HT required for long-term PKA activation, which may correlate with the number of 5HT applications required for LTF. Thus, we further consider the threshold of the number of pulses of 5HT needed for induction of the long-term phase of synaptic facilitation under different time delays. As shown in Fig. 10, the induction of LTF requires three to eight spaced pulses of 5HT when the values of both τ_1 and τ_2 range from 0 to 6 h. Thus, the number of repeated 5HT pulses for LTF can be further regulated by the total value of the time delay in the system.

4 Discussion

Experiments on synaptic plasticity in *Aplysia* confirm that three distinct temporal phases of synaptic facilitation (short-, intermediate-, and long-term) can be induced at the SN-MN synapse by different patterns of 5HT treatment [6, 12]. To probe the mechanisms responsible for the induction of these three stages of facilitation, we develop a multi-scale mathematical model with time delays representing key biochemical processes related to synaptic plasticity involving

regulation of gene expression, presynaptic membrane potential, and EPSP. Bifurcation analysis of the model is performed to reveal the nonlinear dynamics. The two-parameter bifurcation diagram with respect to the stimulus strength and the positive feedback strength is divided into a bistable region and a monostable region by the saddle-node bifurcation curves. For different positive feedback strength, one-parameter bifurcation analysis of the model demonstrates reversible and irreversible bistable switches based on a positive feedback loop. Specifically, the irreversible switch permanently elevates 5HT stimulated PKA at the high stable steady state, which may correlate with the induction of LTF.

The model is validated by confirmation of experimental findings that one or three pulses of 5HT generate short-term phase of PKA activity and STF, and four pulses of 5HT give rise to intermediate-term PKA activation and ITF, whereas five pulses of 5HT lead to both intermediate- and long-term modes of PKA activation and thus ITF and LTF. Notably, the sustained high level of PKA activity after stimulation is due to the positive feedback loop composed of PKA activation and regulation of ApNT expression in the system. Further simulations through repression of translation and transcription in the model demonstrate that the induc-

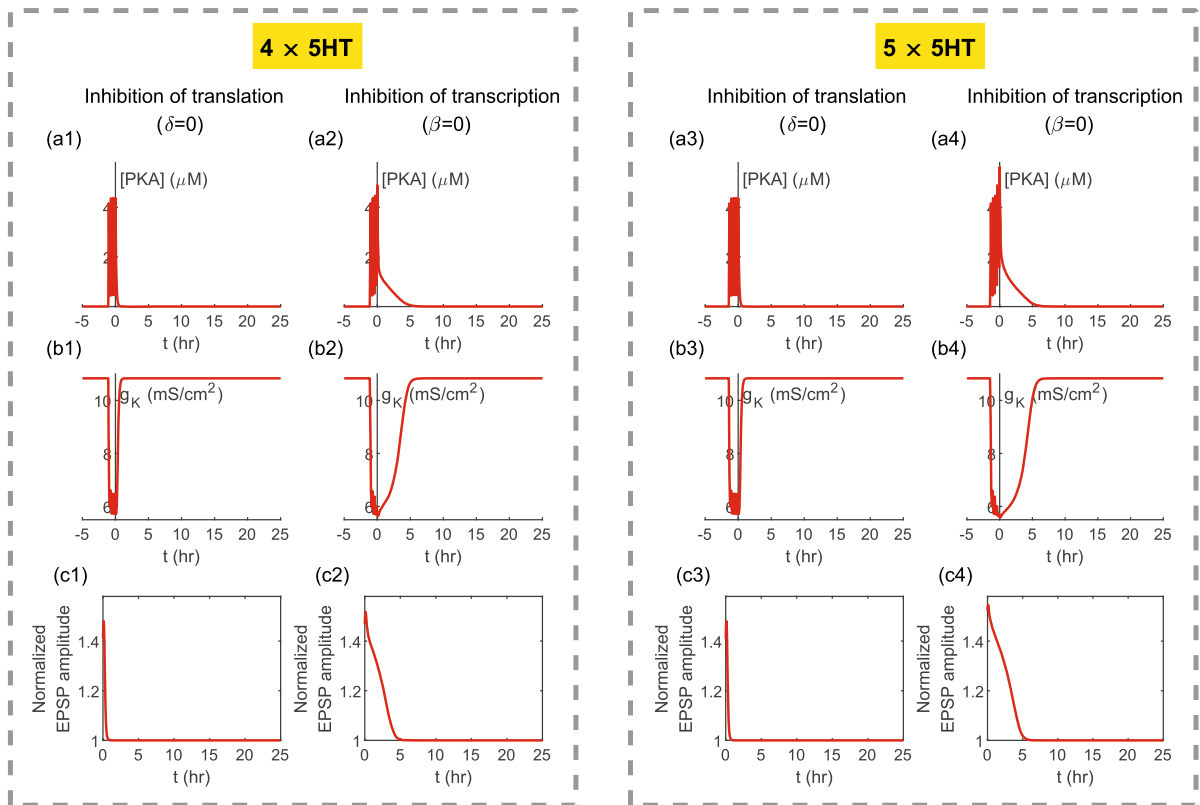


Fig. 8 Time courses of [PKA] (a), g_K (b), and normalized EPSP amplitude (c) after stimulations with four and five pulses of 5HT, with $\delta = 0$ and $\beta = 0$

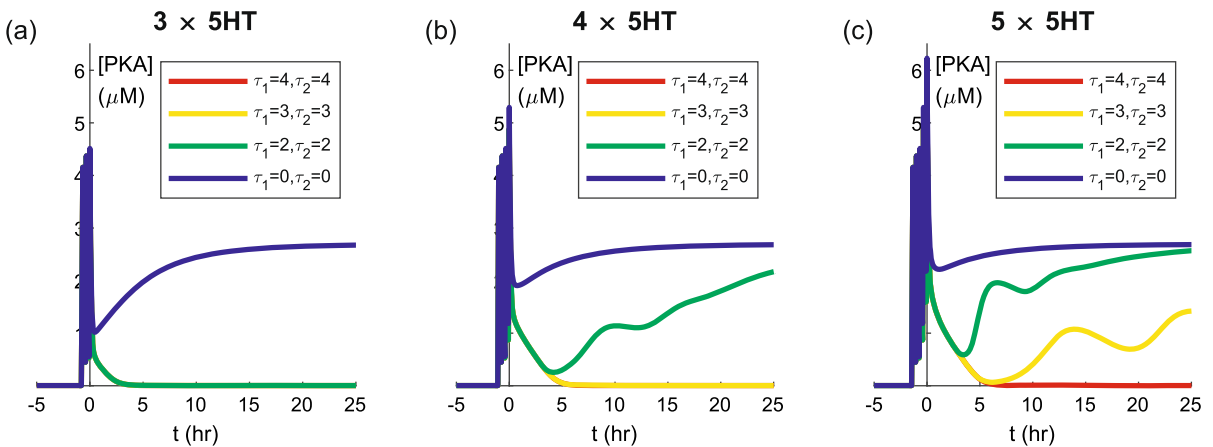


Fig. 9 Time courses of [PKA] following stimulations of three (a), four (b) and five (c) pulses of 5HT at $(\tau_1, \tau_2) = (4 \text{ h}, 4 \text{ h})$ (red), $(\tau_1, \tau_2) = (3 \text{ h}, 3 \text{ h})$ (yellow), $(\tau_1, \tau_2) = (2 \text{ h}, 2 \text{ h})$ (green) and $(\tau_1, \tau_2) = (0 \text{ h}, 0 \text{ h})$ (blue)

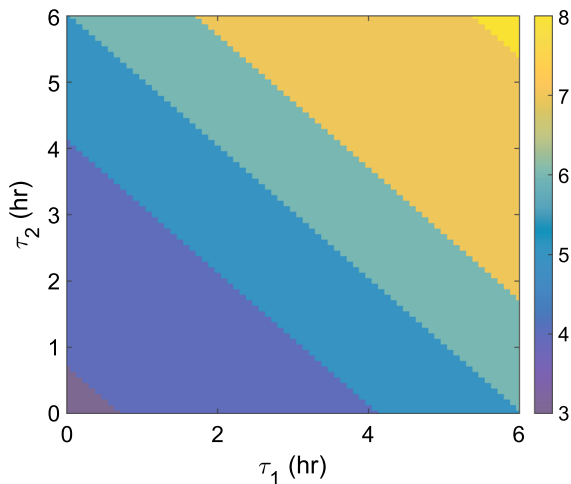


Fig. 10 The threshold number of pulses of 5HT for LTF is dependent on time delays τ_1 and τ_2

tion of STF requires neither mRNA nor protein synthesis, whereas ITF relies on protein but not mRNA synthesis, and LTF depends on both mRNA and protein synthesis. These simulation results are also in line with experimental observations.

Just like different phases of facilitation reported in experimental studies, ITF expressed immediately after 5HT exposure decays to baseline within 3 h, whereas LTF is not expressed before 10 h after 5HT administration. In the model, the delayed onset of LTF can be attributed primarily to the time needed for the synthesis of mRNA and protein. We therefore alter time delays in transcription and translation to determine the threshold of the number of 5HT pulses required for the induction of LTF. We conclude that the pulse number increases with the total values of the time delay. These results signify that the number of repeated 5HT pulses for LTF can be controlled by time delays.

This paper develop a computational model to expound the dynamical mechanisms of SN-MN synapses underlying the induction of three stages of synaptic facilitation in *Aplysia*. The model also provides a framework for understanding other similar processes, and can be used in the biophysical modeling of neural systems for synaptic plasticity, learning and memory. In addition, mathematical modeling and dynamical analysis may establish supporting theories for experimental studies. Accordingly, the model can be used in neuroscience research to connect extensive biophysical processes

associated with synaptic plasticity and reveal the underlying complex dynamics of experimental phenomena.

Recent studies suggest that short-term synaptic plasticity in *Aplysia* is induced by covalent modifications on one side of the synapse, whereas long-term plasticity is expressed by synaptic remodeling involving both sides [30]. Furthermore, the presynaptic positive feedback loop consists of presynaptic PKA and ApNT; a transsynaptic positive feedback loop involving PKA and ApNT in the presynaptic neuron and ApNT in the postsynaptic neuron also contributes to synaptic facilitation at the SN-MN synapse [30]. Our proposed model introduces the presynaptic positive feedback loop but does not consider the transsynaptic one. In future work, we will further investigate both presynaptic and postsynaptic mechanisms and focus on cooperative interactions between them that are essential for synaptic plasticity.

Author contributions LH and ZY designed and performed the research and wrote the article.

Funding This work is supported by the National Natural Science Foundation of China (12372060).

Data availability The data used to support the findings of this study are available from the corresponding author upon request.

Declarations

Conflict of interest All the authors declare that there is no any conflict with the publication of this work.

References

1. Kandel, E.R., Dudai, Y., Mayford, M.R.: The molecular and systems biology of memory. *Cell* **157**(1), 163–186 (2014)
2. Gallero-Salas, Y., Han, S., Sych, Y., Voigt, F.F., Laurenczy, B., Gilad, A., Helmchen, F.: Sensory and behavioral components of neocortical signal flow in discrimination tasks with short-term memory. *Neuron* **109**(1), 135–148 (2021)
3. Roiäast, N.M., Schönauer, M.: Continuously changing memories: a framework for proactive and non-linear consolidation. *Trends Neurosci.* **46**(1), 8–19 (2022)
4. Pronier, É., Morici, J.F., Girardeau, G.: The role of the hippocampus in the consolidation of emotional memories during sleep. *Trends Neurosci.* **46**(11), 912–925 (2023)
5. Seger, S.E., Kriegel, J.L.S., Lega, B.C., Ekstrom, A.D.: Memory-related processing is the primary driver of human hippocampal theta oscillations. *Neuron* **111**(19), 3119–3130 (2023)
6. Maelshagen, J., Parker, G.R., Carew, T.J.: Dynamics of induction and expression of long-term synaptic facilitation in *Aplysia*. *J. Neurosci.* **16**(22), 7099–7108 (1996)

7. Müller, U., Carew, T.J.: Serotonin induces temporally and mechanistically distinct phases of persistent PKA activity in Aplysia sensory neurons. *Neuron* **21**(6), 1423–1434 (1998)
8. Cai, D., Pearce, K., Chen, S., Glanzman, D.L.: Protein kinase M maintains long-term sensitization and long-term facilitation in Aplysia. *J. Neurosci.* **31**(17), 6421–6431 (2011)
9. Jin, I., Kassabov, S., Kandel, E.R., Hawkins, R.D.: Possible novel features of synaptic regulation during long-term facilitation in Aplysia. *Learn. Mem.* **28**(7), 218–227 (2021)
10. Sutton, M.A., Carew, T.J.: Parallel molecular pathways mediate expression of distinct forms of intermediate-term facilitation at tail sensory-motor synapses in Aplysia. *Neuron* **26**(1), 219–231 (2000)
11. Sutton, M.A., Masters, S.E., Bagnall, M.W., Carew, T.J.: Molecular mechanisms underlying a unique intermediate phase of memory in Aplysia. *Neuron* **31**(1), 143–154 (2001)
12. Sherff, C.M., Carew, T.J.: Parallel somatic and synaptic processing in the induction of intermediate-term and long-term synaptic facilitation in Aplysia. *Proc. Natl. Acad. Sci. USA* **101**(19), 7463–7468 (2004)
13. Jin, I., Udo, H., Nicholls, R., Zhu, H., Kandel, E.R., Hawkins, R.D.: Autocrine signaling by an Aplysia neurotrophin forms a presynaptic positive feedback loop. *Proc. Natl. Acad. Sci. USA* **115**(47), E11168–E11177 (2018)
14. Tian, X., Zhang, X., Liu, F., Wang, W.: Interlinking positive and negative feedback loops creates a tunable motif in gene regulatory networks. *Phys. Rev. E* **80**(1), 011926 (2009)
15. Hao, L., Yang, Z.: Mathematical modeling and bistability analysis for synaptic tagging and synapse-specific long-term facilitation in Aplysia. *Eur. Phys. J. Spec. Top.* **231**(5), 963–977 (2022)
16. Maelshagen, J., Sherff, C. M., Carew, T.J.: Differential induction of long-term synaptic facilitation by spaced and massed applications of serotonin at sensory neuron synapses of Aplysia californica. *Learn. Mem.* **5**(3), 246–256 (1998)
17. Gingrich, K.J., Byrne, J.H.: Simulation of synaptic depression, posttetanic potentiation, and presynaptic facilitation of synaptic potentials from sensory neurons mediating gill-withdrawal reflex in Aplysia. *J. Neurophysiol.* **53**(3), 652–669 (1985)
18. Pettigrew, D.B., Smolen, P., Baxter, D.A., Byrne, J.H.: Dynamic properties of regulatory motifs associated with induction of three temporal domains of memory in Aplysia. *J. Comput. Neurosci.* **18**(2), 163–181 (2005)
19. Zhou, L., Baxter, D.A., Byrne, J.H.: Contribution of PKC to the maintenance of 5-HT-induced short-term facilitation at sensorimotor synapses of Aplysia. *J. Neurophysiol.* **112**(8), 1936–1949 (2014)
20. Hao, L., Yang, Z., Shen, D., Xing, M.: From reversible to irreversible bistable switches via bifurcations in a gene regulatory network. *Phys. Biol.* **17**(4), 046001 (2020)
21. Hao, L., Yang, Z.: Dynamical mechanisms for gene regulation mediated by two noncoding RNAs in long-term memory formation. *Neural Plast.* **2021**, 6668389 (2021)
22. Hao, L., Yang, Z., Bi, Y.: Deterministic and stochastic dynamics in a gene regulatory network mediated by miRNA. *Nonlinear Dyn.* **103**(3), 2903–2916 (2021)
23. Kandel, E.R.: The molecular dialogue biology of memory and storage: synapses between genes. *Science* **294**(5544), 1030–1038 (2001)
24. Martin, K.C., Casadio, A., Zhu, H., Yaping, E., Rose, J.C., Chen, M., Bailey, C.H., Kandel, E.R.: Synapse-specific, long-term facilitation of Aplysia sensory to motor synapses: a function for local protein synthesis in memory storage. *Cell* **91**(7), 927–938 (1997)
25. Santos, A.R., Comprido, D., Duarte, C.B.: Regulation of local translation at the synapse by BDNF. *Prog. Neurobiol.* **92**(4), 505–516 (2010)
26. Gao, L., Zhang, Y., Sterling, K., Song, W.: Brain-derived neurotrophic factor in Alzheimer’s disease and its pharmaceutical potential. *Transl. Neurodegener.* **11**(1), 4 (2022)
27. Tokunaga, N., Takimoto, T., Nakamura, Y., Hisaoka-Nakashima, K., Morioka, N.: Downregulation of connexin 43 potentiates amitriptyline-induced brain-derived neurotrophic factor expression in primary astrocytes through lysophosphatidic acid receptor_{1/3}, Src, and extracellular signal-regulated kinase. *Eur. J. Pharmacol.* **925**, 174986 (2022)
28. Park, H., Poo, M.-M.: Neurotrophin regulation of neural circuit development and function. *Nat. Rev. Neurosci.* **14**(1), 7–23 (2013)
29. Hao, L., Yang, Z., Lei, J.: Underlying mechanisms of cooperativity, input specificity, and associativity of long-term potentiation through a positive feedback of local protein synthesis. *Front. Comput. Neurosci.* **12**, 25 (2018)
30. Jin, I., Udo, H., Kassabov, S., Kosmidis, S., Zhu, H., Kandel, E.R., Hawkins, R.D.: Anterograde and retrograde signaling by an Aplysia neurotrophin forms a transsynaptic functional unit. *Proc. Natl. Acad. Sci. USA* **115**(46), E10951–E10960 (2018)
31. Morris, C., Lecar, H.: Voltage oscillations in the barnacle giant muscle fiber. *Biophys. J.* **35**(1), 193–213 (1981)
32. Ermentrout, B.: *Simulating, Analyzing, and Animating Dynamical Systems: A Guide to XPPAUT for Researchers and Students.* SIAM (2003)

Publisher’s Note Springer Nature remains neutral with regard to jurisdictional claims in published maps and institutional affiliations.

Springer Nature or its licensor (e.g. a society or other partner) holds exclusive rights to this article under a publishing agreement with the author(s) or other rightsholder(s); author self-archiving of the accepted manuscript version of this article is solely governed by the terms of such publishing agreement and applicable law.